# Statistical properties of non-linear Froude-Krylov forces on cylinders

*Felice Arena and Francesco Fedele*
Department of Mechanics and Materials, University 'Mediterranea' of Reggio Calabria
Via Graziella, loc. Feo di Vito – 89100 Reggio Calabria – Italy – E-mail: arena@unirc.it

**ABSTRACT**

**The statistical properties of the second-order Froude-Krylov force on a cylinder (whether a vertical cylinder or a horizontal submerged cylinder), for narrow-band spectra, are investigated. For this purpose two families of stochastic processes are defined and for each family the probability density function and the probabilities of exceedance of the absolute maximum and of the absolute minimum are obtained. It is then proven that the above-mentioned Froude-Krylov force processes belong to these stochastic families.**
**The predictions for the Froude-Krylov force on a horizontal submerged cylinder agree with the results of a small-scale field experiment.**

**KEY WORDS**

Random wind-generated waves. Froude-Krylov force. Non-linearity effects. Probability of exceedance of the absolute maximum. Probability of exceedance of the absolute minimum. Vertical cylinder. Horizontal submerged cylinder.

**INTRODUCTION**

The amplitude of the wave force on a large structure may be obtained as the product of the Froude-Krylov force (which is defined as the force on the equivalent water volume) and the diffraction coefficient of the wave force (Sarpkaya and Isaacson, 1981). Therefore it is helpful for the design of large offshore structures to investigate the properties of the Froude-Krylov force.

According to the linear theory of wind-generated waves (Longuet-Higgins, 1963; Phillips, 1967) the linear Froude-Krylov force, whether on a vertical cylinder or on a horizontal submerged cylinder, represents a random Gaussian process of time. Therefore both the absolute maximum and the absolute minimum of the linear Froude-Krylov force have the same Rayleigh distribution, if the spectrum is very narrow (Longuet-Higgins, 1952).

Boccotti (2000) has shown that, for large horizontal cylinders, the two random processes *wave force on the solid cylinder*, and *Froude-Krylov wave force* have nearly the same very narrow spectrum, the same non-linearity effects, and the same statistical properties: equal distribution of the normalized crest-to-trough heights, distribution of the normalized absolute maximum and distribution of the normalized absolute minimum. This conclusion is based on the evidence of a small-scale field experiment which consisted in the real time comparison of the wave forces on a horizontal submerged cylinder and on an ideal equivalent water cylinder (see also Boccotti, 1996).

This paper deals with the statistical properties of the non-linear Froude-Krylov forces exerted by narrow-band wind-generated waves (Tayfun, 1980). For this purpose we define two families of non-linear stochastic processes $\psi_1$ and $\psi_2$: the first consisting of statistically symmetric processes, the second consisting of statistically non-symmetric processes. For each family of random processes we obtain the probability density function, the probability of exceedance of the absolute maximum and the probability of exceedance of the absolute minimum. For the family $\psi_1$ these properties depend upon one parameter $\delta$, for the family $\psi_2$ they depend upon two parameters $\alpha_1$ and $\alpha_2$.

We prove that the horizontal component of the narrow-band second-order Froude-Krylov force (whether on a vertical cylinder or on a horizontal submerged cylinder) represents a random process of time which belongs to the stochastic family $\psi_1$, and the expression of parameter $\delta$ is derived for this process. We prove also that the vertical component of the narrow-band second-order Froude-Krylov force (on a horizontal submerged cylinder) represents a random process of time which belongs to the stochastic family $\psi_2$ and the expressions of parameters $\alpha_1$ and $\alpha_2$ are obtained for this process.

Finally, we show that the analytical predictions for the Froude-Krylov force on a horizontal submerged cylinder agree with the conclusions of Boccotti (2000) based on experimental evidence.

**STATISTICAL PROPERTIES OF TWO STOCHASTIC FAMILIES WITH NARROW-BAND SPECTRUM**

Let us define the two families of stochastic processes of time:

$$\psi_1(t) = f_1 a \sin[\chi(t)] + g_1 a^2 \sin[2\chi(t)]\,, \tag{1}$$

$$\psi_2(t) = f_2\, a \cos[\chi(t)] + g_2 a^2 \cos^2[\chi(t)] + h_2 a^2 \sin^2[\chi(t)]\,, \tag{2}$$

where $a$ is a Rayleigh distributed random variable, $f_1$, $g_1$, $f_2$, $g_2$,

$h_2$ are parameters with some fixed values and where

$$\chi(t) = wt + \varphi \,, \tag{3}$$

with $w$ the angular frequency and $\varphi$ a random phase uniformly distributed in $(0,2\pi)$.

**The probability density functions of the stochastic family $\psi_1$**

Let us consider the normalized random process

$$\zeta_1 = \frac{\psi_1 - \overline{\psi_1}}{\sigma_{\psi_1}} \tag{4}$$

where $\overline{\psi_1}$ and $\sigma_{\psi_1}$ are, respectively, the mean value and the standard deviation of random process $\psi_1$. Defining the two Gaussian random processes of time

$$Z_c(t) = \frac{a\cos[\chi(t)]}{\sigma}, \quad Z_s(t) = \frac{a\sin[\chi(t)]}{\sigma} \tag{5}$$

where $\sigma$ is the standard deviation of the linear process $a\sin[\chi(t)]$, the normalized process $\zeta_1$ may be rewritten as

$$\zeta_1 = \nu Z_s + (\delta/\nu) Z_c Z_s \tag{6}$$

where

$$\nu = 1\Big/\sqrt{1+\delta^2/4} \qquad \delta = 2g_1\sigma\big/|f_1|\,, \tag{7}$$

given that

$$\overline{\psi_1} = 0, \qquad \sigma^2_{\psi_1} = \sigma^2\left(f_1^2 + \sigma^2 g_1^2\right). \tag{8}$$

The third and fourth moments of the family $\zeta_1$, are given respectively by:

$$\overline{\zeta_1^3} = 0\,, \tag{9}$$

$$\overline{\zeta_1^4} = 3\nu^4 + 18\delta^2 + 9(\delta/\nu)^2\,. \tag{10}$$

The vanishing of the third moment suggests that $\zeta_1$ is a symmetric process. To show this symmetry the probability density function of $\zeta_1$ is derived. Firstly we evaluate the characteristic function of the process $\zeta_1$, which is defined as the mean value of $e^{i\omega\zeta_1}$:

$$\overline{e^{i\omega\zeta_1}} = \int_{-\infty}^{+\infty}\int_{-\infty}^{+\infty} e^{i\omega\zeta_1} f_{Z_1,Z_2}(z_1,z_2)\,\mathrm{d}z_1\mathrm{d}z_2 = \frac{1}{2\pi}\int_{-\infty}^{+\infty} e^{-\frac{1}{2}z_1^2} I_1(z_1)\,\mathrm{d}z_2\,, \tag{11}$$

where $f_{Z_1,Z_2}$ is the bi-variate Gaussian probability density function ($Z_1, Z_2$ are independent random variable of time) and the integral $I_1$ is defined as

$$I_1 = \mathbf{L}\left(\cos(\lambda\sqrt{t})/\sqrt{t}, s = 1/2\right), \quad \lambda = \omega\left(\nu + \delta/\nu z_1\right), \tag{12}$$

where the Laplace transform is given by

$$\mathbf{L}\left(\cos(\lambda\sqrt{t})/\sqrt{t}, s\right) = \sqrt{\pi/s}\,\exp[-\lambda^2/(4s)]\,. \tag{13}$$

Substitution in Eq. 11 and some algebra give us

$$\overline{e^{i\omega\zeta_1}} = \frac{e^{-\frac{1}{2}\omega^2}}{\sqrt{2\pi}}\,\mathbf{L}\left(\frac{\cos(i\omega^2\delta\sqrt{t})}{\sqrt{t}}; s = \frac{1}{2}\left(\nu^2 + \omega^2\delta^2/\nu^2\right)\right) \tag{14}$$

and finally the characteristic function results

$$\overline{e^{i\omega\zeta_1}} = \exp\left[-\frac{1}{2}\omega^2\left(1 - \frac{\delta^2\omega^2}{\nu^2 + \omega^2\delta^2/\nu^2}\right)\right]\Big/\sqrt{\nu^2 + \omega^2\delta^2/\nu^2}\,. \tag{15}$$

The probability density function of $\zeta_1$ is obtained by inverse Fourier transform of $\overline{e^{i\omega\zeta}}$ (Eq. 15):

$$f_{\zeta_1}(\zeta) = \mathbf{F}^{-1}\left(\overline{e^{i\omega\zeta}}, \zeta\right) = \frac{1}{2\pi}\int_{-\infty}^{+\infty} e^{-i\omega\zeta}\,\overline{e^{i\omega\zeta}}\,\mathrm{d}\omega\,, \tag{16}$$

in which $\mathbf{F}^{-1}$ is the inverse-Fourier transform operator. The Eq. 16 leads the general expression of $f_{\zeta_1}$:

$$f_{\zeta_1}(\zeta) = \frac{1}{\pi}\int_0^{+\infty} \cos(\omega\zeta)\frac{\exp\left[-\frac{1}{2}\omega^2\left(1 - \frac{\delta^2\omega^2}{\nu^2 + \omega^2\delta^2/\nu^2}\right)\right]}{\sqrt{\nu^2 + \omega^2\delta^2/\nu^2}}\,\mathrm{d}\omega\,. \tag{17}$$

Note that this probability density function is symmetric with respect to $\zeta = 0$, which means that the random process $\zeta_1$ is statistically symmetric. Note also that the probability density function $f_{\zeta_1}$ (Eq. 17) of the normalized random variable $\zeta_1$ approaches the probability density function of the normalized Gaussian variable, as $\delta$ approaches zero. Figure 1 compares the $f_{\zeta_1}$ for two values of $\delta$ and the probability density function of the normalized Gaussian random variable.

**The probability density functions of the stochastic family $\psi_2$**

Let us consider the normalized random process

$$\zeta_2 = \frac{\psi_2 - \overline{\psi_2}}{\sigma_{\psi_2}} \tag{18}$$

where $\overline{\psi_2}$ and $\sigma_{\psi_2}$ are, respectively, the mean value and the standard deviation of random process $\psi_2$. As function of the processes $Z_c$ and $Z_s$ (see Eq. 5), the process $\zeta_2$ may be written as

$$\zeta_2 = \beta\left(Z_c + \alpha_1 Z_c^2 + \alpha_2 Z_s^2\right) - \beta\left(\alpha_1 + \alpha_2\right), \tag{19}$$

where

$$\alpha_1 = \sigma\frac{g_2}{|f_2|}, \quad \alpha_2 = \sigma\frac{h_2}{|f_2|}, \quad \beta = \frac{1}{\sqrt{1 + 2(\alpha_1^2 + \alpha_2^2)}}\,, \tag{20}$$

given that

$$\overline{\psi_2} = f_2\,\sigma(\alpha_1 + \alpha_2)\,, \quad \sigma^2_{\psi_2} = \sigma^2 f_2^2/\beta^2\,. \tag{21}$$

The third and fourth moments of the family $\zeta_2$ are given respectively by:

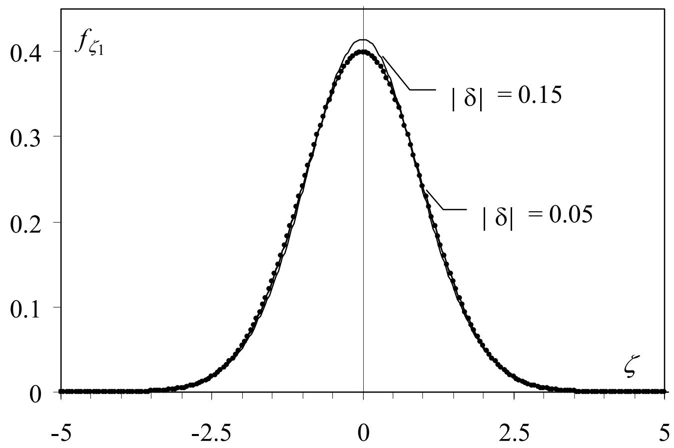


Figure 1. Comparison between the probability density functions $f_{\zeta_1}$ (Eq. 17), for fixed values of $\delta$, and the normalized Gaussian (dotted line).

$$\overline{\zeta_2^3} = \beta^3(6\alpha_1 + 8\alpha_1^3 + 8\alpha_2^3)\,, \tag{22}$$

$$\overline{\zeta_2^4} = 3\beta^4(1 + 20\alpha_1^2 + 4\alpha_2^2 + 20\alpha_1^4 + 8\alpha_1^2\alpha_2^2 + 20\alpha_2^4)\,. \tag{23}$$

Therefore the family $\zeta_2$ is generally non-symmetric.
The characteristic function of $\zeta_2$ is given by

$$\overline{e^{i\omega\zeta_2}} = \frac{1}{2\pi}e^{-i\omega\beta(\alpha_1+\alpha_2)}\,\mathcal{L}\left(\frac{\cos\left(\omega\beta\sqrt{t}\right)}{\sqrt{t}}, s = \frac{1-2i\omega\beta\alpha_1}{2}\right)\cdot \mathcal{L}\left(\frac{e^{i\omega\beta\alpha_2 t}}{\sqrt{t}}, s = \frac{1}{2}\right) \tag{24}$$

and by using both the Eq. 13 and the Laplace transform

$$\mathcal{L}\left(\frac{e^{\lambda t}}{\sqrt{t}}, s\right) = \mathcal{L}\left(\frac{1}{\sqrt{t}}, s-\lambda\right) = \frac{\sqrt{\pi}}{\sqrt{s-\lambda}}\,, \tag{25}$$

the characteristic function 24 is given by

$$\overline{e^{i\omega\zeta_2}} = \left\{\exp\left[-\frac{1}{2}\frac{(\omega\beta)^2}{1+4(\omega\beta\alpha_1)^2}\right]\exp\left[-i\omega\beta\left((\alpha_1+\alpha_2) + \frac{(\omega\beta)^2\alpha_1}{1+4(\omega\beta\alpha_1)^2}\right)\right]\right\}\Bigg/\sqrt{1-4(\omega\beta)^2\alpha_1\alpha_2 - 2i\omega\beta(\alpha_1+\alpha_2)}\,. \tag{26}$$

Finally, the probability density function $f_{\zeta_2}$ is obtained by applying the inverse Fourier transform to the characteristic function $\overline{e^{i\omega\zeta_2}}$, that is:

$$f_{\zeta_2}(\zeta) = \frac{1}{2\pi}\int_{-\infty}^{+\infty} \mathrm{e}^{-i\omega\zeta}\exp\left[-\frac{1}{2}\frac{(\omega\beta)^2}{1+4(\omega\beta\alpha_1)^2}\right]\cdot \frac{\exp\left\{-i\omega\beta\left[(\alpha_1+\alpha_2) + \frac{(\omega\beta)^2\alpha_1}{1+4(\omega\beta\alpha_1)^2}\right]\right\}}{\sqrt{1-4(\omega\beta)^2\alpha_1\alpha_2 - 2i\omega\beta(\alpha_1+\alpha_2)}}\,\mathrm{d}\omega. \tag{27}$$

Let us observe that if the parameters $\alpha_1, \alpha_2$ approach zero, the non-linearity vanishes and the probability density function of $\zeta_2$ (Eq. 27) tends to the Gaussian distribution.
Figure 2 shows the probability density function $f_{\zeta_2}$ (Eq. 27), for fixed values of ( $\alpha_1, \alpha_2$ ).

**The probabilities of exceedance of the absolute maximum and of the absolute minimum of the stochastic family $\psi_1$**

Being the family $\psi_1$ (Eq. 1) symmetric, the distribution of the absolute maximum is equal to the distribution of the absolute minimum. Therefore we derive only the probability of exceedance of the absolute maximum.
If we rewrite the normalized process $\zeta_1$ (Eq. 6) as

$$\zeta_1 = \frac{\nu a}{\sigma}\sin(\chi) + \frac{1}{2}\frac{\delta}{\nu}\left(\frac{a}{\sigma}\right)^2\sin(2\chi)\,. \tag{28}$$

the first derivative $\mathrm{d}\zeta_1/\mathrm{d}\chi$ vanishes if

$$2\mu\cos^2\chi + \cos\chi - \mu = 0\,. \tag{29}$$

where

$$\mu \equiv \delta\, a/(\nu^2\sigma)\,. \tag{30}$$

In the following we analyze the roots of Eq. 29 in the domain of the parameter $\mu$. If $\mu \to 0$ the effects of non-linearity are negligible and Eq. 29 reduces itself to $\cos\chi = 0$ : the abscissa $\chi = \pi/2$ of the maximum value is equal to the maximum abscissa for the linear process $\zeta_{1L} = (\nu a/\sigma)\sin(\chi)$. If $\mu \to \infty$ the non-linearity is predominant and Eq. 29 reduces itself to $\cos^2\chi = 1/2$ : the abscissa of the maximum value is $\chi = \pi/4$. For finite $\mu$, the abscissa of the maximum is within $\pi/4$ and $\pi/2$ and Eq. 29 is satisfied if

$$\cos\chi_{\max} = \frac{4\mu}{1+\sqrt{1+32\mu^2}}\,, \qquad \sin\chi_{\max} > 0\,. \tag{31}$$

If we assume weak non-linear effects (that is $\mu << 1$ ), for a fixed value of $a/\sigma$, Eq. 31 may be expanded in Taylor series as

$$\cos\chi_{\max} \cong 2\mu - 16\mu^2 \qquad \sin\chi_{\max} \cong 1 - 2\mu^2\,. \tag{32}$$

Substitution of expressions 32 in Eq. 28, after some algebra, by retaining only the lower order terms, gives us the approximate expression for the maximum

$$\zeta_{1\max} = \zeta_1(\chi_{\max}) \cong \nu u + \frac{\delta^2}{2\nu^3}u^3\,. \tag{33}$$

Successive approximations procedure yields the following expressions for $u_0$ such that Eq. 33 is satisfied

$$u_0 \cong \frac{\zeta_{1\max}}{\nu} - \frac{\delta^2}{2\nu^7}\zeta_{1\max}^3 \tag{34}$$

and the probability of exceedance for the absolute maximum has expression

$$P(\zeta_{1\max} > \zeta) = \Pr\left[u > \frac{\zeta}{\nu} - \frac{\delta^2}{2\nu^7}\zeta^3\right]. \tag{35}$$

Having the variable $u$ the Rayleigh distribution (that is $P(u \geq z) = \exp(-z^2/2)$ ) the Eq. 35 becomes:

$$P(\zeta_{1\max} > \zeta) = \exp\left[-\frac{1}{2}\zeta^2\left(\frac{1}{\nu} - \frac{\delta^2}{2\nu^7}\zeta^2\right)^2\right]. \tag{36}$$

This probability of exceedance, for fixed values of $\delta$, is shown in Figure 3. Let us note that the deviation from the Rayleigh distribution is weak for $|\delta| < 0.05$.

**The probabilities of exceedance of the absolute maximum and of the absolute minimum of the stochastic family $\psi_2$**

To achieve the distribution of the absolute maximum and the distribution of the absolute minimum of the stochastic family $\psi_2$, it is convenient to rewrite the Eq. 2 as the following form:

$$\psi_2(x,z) = f_2(x,z)a\cos(\chi) + [g_2(x,z) - h_2(x,z)]\frac{a^2}{2}\cos(2\chi) + [g_2(x,z) + h_2(x,z)]\frac{a^2}{2}. \tag{37}$$

The first derivative of $\psi_2$ is given by:

$$\frac{\mathrm{d}\psi_2}{\mathrm{d}\chi} = -a\sin(\chi)\{f_2(x,z) + 2[g_2(x,z) - h_2(x,z)]a\cos(\chi)\}, \tag{38}$$

and vanishes if

$$\sin(\chi) = 0 \tag{39}$$

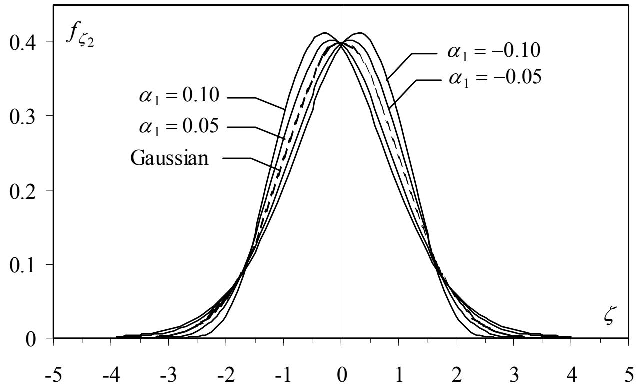


Figure 2. The probability density functions $f_{\zeta_2}$ (Eq. 27), for fixed values of $\alpha_1$ (it has been assumed $\alpha_2 = -\alpha_1$). The dashed line is the Gaussian distribution, obtained for $\alpha_1$=0.

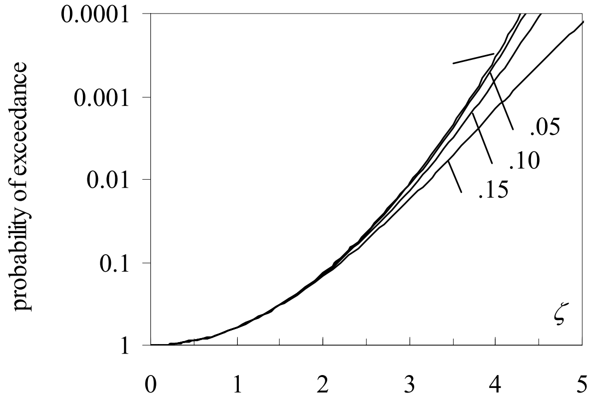


Figure 3. The probability of exceedance $P(\zeta_{1\max} > \zeta)$ of the absolute maximum (Eq. 36), for fixed $|\delta|$. The probability $P(\zeta_{1\max} > \zeta)$ is equal to the Rayleigh distribution for $\delta$=0.

or, for the general case of $g_2(x,z) \neq h_2(x,z)$, if

$$\cos(\chi) = -\frac{f_2(x,z)}{2[g_2(x,z) - h_2(x,z)]a} . \tag{40}$$

Assuming that Eq. 40 has no solution, the unique stationary points of $\psi_2$ are the stationary points of the linear process $\psi_{2L}(x,z) = f_2(x,z) a \cos(\chi)$ (this condition is satisfied if the ratio between the amplitude of the linear component and the amplitude of the non-linear component is greater than 4).

Therefore if $f_2 < 0$ the abscissa of the absolute maximum is given by $\chi_{\max} = \pi$ and the abscissa of the absolute minimum is given by $\chi_{\min} = 0$. The amplitudes of the absolute maximum and of the absolute minimum (in absolute value) are given respectively by:

$$\Psi_{2\max} = -f_2(x,z)a + g_2(x,z)a^2 , \tag{41}$$

$$\Psi_{2\min} = -f_2(x,z)a - g_2(x,z)a^2 . \tag{42}$$

Let us define the dimensionless variables:

$$\zeta_{2\max} = \frac{\Psi_{2\max}}{\sigma_{\psi_2}} = u\beta + \alpha_1 \beta u^2 , \quad \zeta_{2\min} = \frac{\Psi_{2\min}}{\sigma_{\psi_2}} = u\beta - \alpha_1 \beta u^2 \tag{43}$$

where $\beta$, $\alpha_1$ and $\alpha_2$ are defined by Eq. 20 and where the random variable $u$ has Rayleigh distribution. Therefore the probabilities of exceedance of the absolute maximum $P(\zeta_{2\max} > \zeta)$ and of the absolute minimum $P(\zeta_{2\min} > \zeta)$ are given by

if $\alpha_1 > 0$ :

$$\begin{cases} P(\zeta_{2\max} > \zeta) = f_a(\zeta), \\ P(\zeta_{2\min} > \zeta) = \begin{cases} f_b(\zeta) & \text{if} \quad \zeta \le \beta/(4|\alpha_1|), \\ 0 & \text{if} \quad \zeta > \beta/(4|\alpha_1|), \end{cases} \end{cases} \tag{44}$$

if $\alpha_1 < 0$ :

$$\begin{cases} P(\zeta_{2\max} > \zeta) = \begin{cases} f_b(\zeta) & \text{if} \quad \zeta \le \beta/(4|\alpha_1|), \\ 0 & \text{if} \quad \zeta > \beta/(4|\alpha_1|), \end{cases} \\ P(\zeta_{2\min} > \zeta) = f_a(\zeta), \end{cases} \tag{45}$$

where the functions $f_a$ and $f_b$ are respectively:

$$f_a(\zeta) = \exp\left[ -\left(1 - \sqrt{1 + 4|\alpha_1|\zeta/\beta}\right)^2 \Big/ \left(8\alpha_1^2\right) \right] , \tag{46}$$

$$f_b(\zeta) = \exp\left[ -\left(1 - \sqrt{1 - 4|\alpha_1|\zeta/\beta}\right)^2 \Big/ \left(8\alpha_1^2\right) \right] + \\ - \exp\left[ -\left(1 + \sqrt{1 - 4|\alpha_1|\zeta/\beta}\right)^2 \Big/ \left(8\alpha_1^2\right) \right] \tag{47}$$

(the parameters $\alpha_1$, $\alpha_2$ and $\beta$ are defined by Eq. 20).

Figure 4 shows the probabilities of exceedance $P(\zeta_{2\max} > \zeta)$ of the absolute maximum and $P(\zeta_{2\min} > \zeta)$ of the absolute minimum for fixed values of $\alpha_1$ (and for $|\alpha_2| = \alpha_1$). Observe that for $\alpha_1$ approaching zero both the probabilities of exceedance reduce themselves to the Rayleigh distribution. For $\alpha_1 \neq 0$ the two distributions are different: in particular for a fixed threshold of the probability of exceedance, if $\alpha_1 > 0$ the absolute maximum is greater than the absolute minimum [and therefore each realization of the process is a sequence of waves which have crest amplitude (absolute maximum) greater than the trough amplitude (absolute minimum)]; if $\alpha_1 < 0$ the absolute minimum is greater than the absolute maximum (and therefore each realization of the process is a sequence of waves which have the trough amplitude greater than the crest amplitude). It is also easy to verify that the distributions of Figure 4 are not modified if $\alpha_2$ ranges between $-|\alpha_1|$ and $|\alpha_1|$.

## APPLICATIONS

Let us assume the reference frame $(x, y, z)$ with the $x$-axis horizontal (direction along which the waves attack), the $y$-axis horizontal and the $z$-axis vertical with origin at the mean water level, as well as $d$ the bottom depth.

The narrow-band second-order Froude-Krylov force processes, both for a vertical cylinder and for a horizontal submerged cylinder, are derived by analytical integration of the narrow-band second-order wave pressure.

The steepness $\varepsilon$ (being $\varepsilon = k\sigma$, $k$ the wave number and $\sigma$ the standard deviation of the linear surface displacement) ranges typically between 0.05 and 0.08.

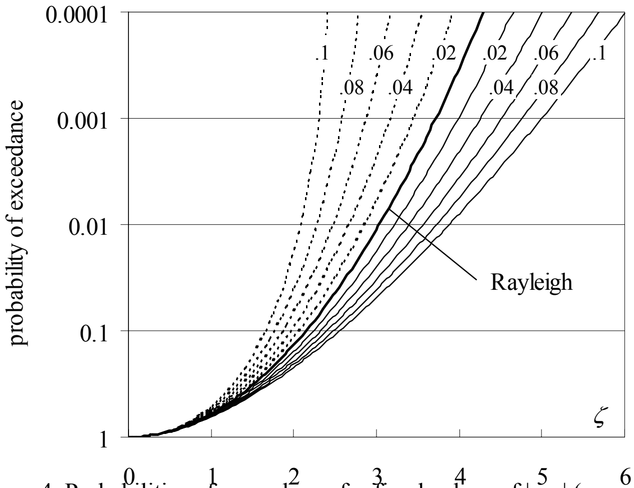


Figure 4. Probabilities of exceedance for fixed values of $|\alpha_1|$ (assuming that $|\alpha_2|=|\alpha_1|$). (i) Positive $\alpha_1$ : continuous lines are the absolute maximum distribution $P(\zeta_{2\max} > \zeta)$ , dashed lines are the absolute minimum distribution $P(\zeta_{2\min} > \zeta)$ . (ii) Negative $\alpha_1$ : continuous lines are the $P(\zeta_{2\min} > \zeta)$ , dashed lines are the $P(\zeta_{2\max} > \zeta)$

The second-order random wave pressure in an undisturbed field, for a narrow spectrum, is given by

$$\Delta p(x,z,t) = \rho g a \frac{\cosh[k(z+d)]}{\cosh(kd)} \cos(kx - wt - \varphi) + $$
$$+ \rho g k a^2 \frac{3\cosh[2k(z+d)] - \sinh^2(kd)}{4\sinh^3(kd)\cosh(kd)} \cos[2(kx - wt - \varphi)] + \quad (48)$$
$$- \rho g k a^2 \frac{\cosh[2k(z+d)] - 1}{2\sinh(2kd)},$$

and belongs to the stochastic family $\psi_2$ (Arena and Fedele, 2000*a*).

**The narrow-band second-order Froude-Krylov force on a vertical cylinder**

*The sectional force*

Let us consider an ideal water vertical cylinder with radius $R$ (see Figure 5). The Froude-Krylov force (force for unitary lenght), at a fixed level $z$, is given by

$$F_x(z) = -\int_0^{2\pi} R\,\Delta p(R,\theta,z)\cos(\theta)\,\mathrm{d}\theta \quad (49)$$

(we consider the variable transformation $x = r\cos\theta; y = r\sin\theta$ - see Figure 5).
From expression 48 for the wave pressure, the narrow-band horizontal component of the Froude-Krylov force (see Eq. 49), is given by

$$F_x(z) = -\rho g R a \frac{\cosh[k(z+d)]}{\cosh(kd)} \int_0^{2\pi} \cos(kR\cos\theta - wt - \varphi)\cdot$$
$$\cdot \cos\theta\,\mathrm{d}\theta - \rho g k R a^2 \frac{3\cosh[2k(z+d)] - \sinh^2(kd)}{4\sinh^3(kd)\cosh(kd)} \cdot \quad (50)$$
$$\cdot \int_0^{2\pi} \cos[2(kR\cos\theta - wt - \varphi)]\cos\theta\,\mathrm{d}\theta .$$

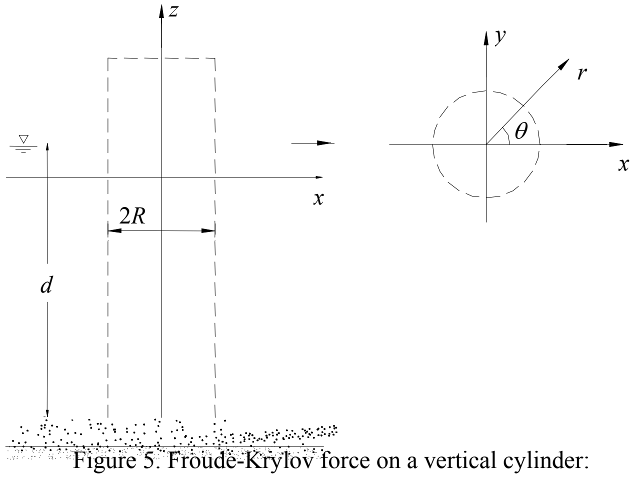


Figure 5. Froude-Krylov force on a vertical cylinder: the reference frame.

The solution of the integrals in Eq. 50 leads

$$F_x(z) = -\rho g\, 2\pi R a J_1(kR) \frac{\cosh[k(z+d)]}{\cosh(kd)} \sin(wt+\varphi) - \rho g\, 2\pi kR \cdot$$
$$\cdot a^2 J_1(2kR) \frac{3\cosh[2k(z+d)] - \sinh^2(kd)}{4\sinh^3(kd)\cosh(kd)} \sin[2(wt+\varphi)]. \quad (51)$$

The process $F_x$ (Eq. 51) belongs to the symmetric family $\psi_1$ with parameter

$$\delta = -\varepsilon \frac{J_1(2kR)}{|J_1(kR)|} \frac{3\cosh[2k(z+d)] - \sinh^2(kd)}{2\sinh^3(kd)\cosh[k(z+d)]} \quad (52)$$

in which $J_1(x)$ is the Bessel function of the first kind.

*The total force*

The total force, which is defined as

$$F_x = \int_{-h}^{0} F_x(z)\,\mathrm{d}z , \quad (53)$$

is given by

$$F_x = -\rho g\, 2\pi R d a J_1(kR) \frac{\tanh(kd)}{kd} \sin(wt+\varphi) +$$
$$- \rho g 2\pi kR d a^2 J_1(2kR) \frac{3\dfrac{\sinh(2kd)}{2kd} - \sinh^2(kd)}{4\sinh^3(kd)\cosh(kd)} \cdot \quad (54)$$
$$\cdot \sin[2(wt+\varphi)].$$

This process belongs to the family $\psi_1$ (Eq. 1) with parameter

$$\delta = -\varepsilon \frac{J_1(2kR)}{|J_1(kR)|} \frac{3\sinh(2kd) - 2kd\sinh^2(kd)}{4\sinh^4(kd)} . \quad (55)$$

In Figure 6 the projection of the parameter $\delta/\varepsilon$ as function of $kR$ is shown, for fixed values of $kd$ . Let us note that the parameter $\delta$ decreases as the depth increases; it is also small: for $kd > 1.5$ we have $|\delta| < 0.5\varepsilon$ (that is $|\delta| < 0.025 \div 0.04$ ).
Therefore the second-order Froude-Krylov force on a vertical cylinder (Eq. 54), for a narrow-band spectrum, is a symmetric quasi-Gaussian process; as a consequence the probabilities of exceedance of the absolute maximum and of the absolute minimum are very close to the Rayleigh distribution (compare to Figure 3).

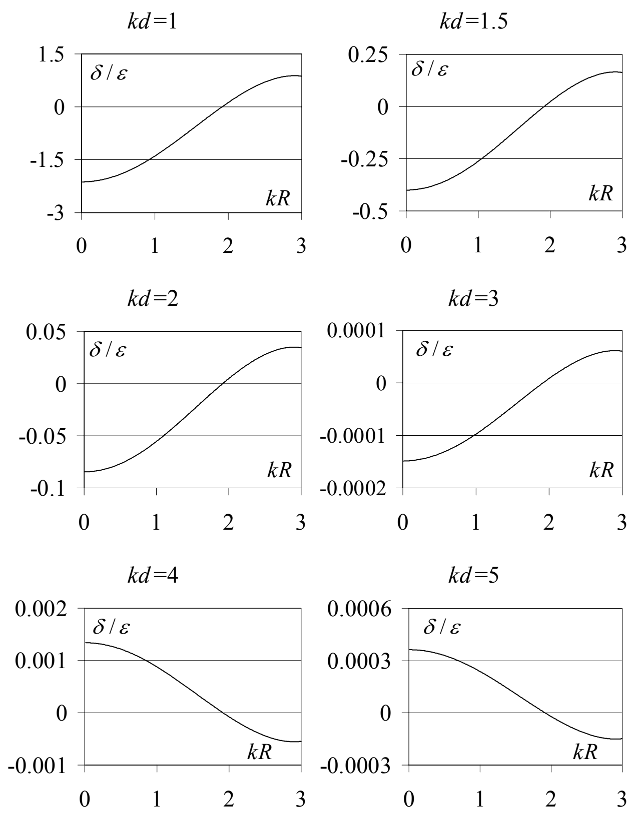


Figure 6. Froude-Krylov force on a vertical cylinder: the parameter $\delta / \varepsilon$ as function of $kR$, for fixed values of $kd$.

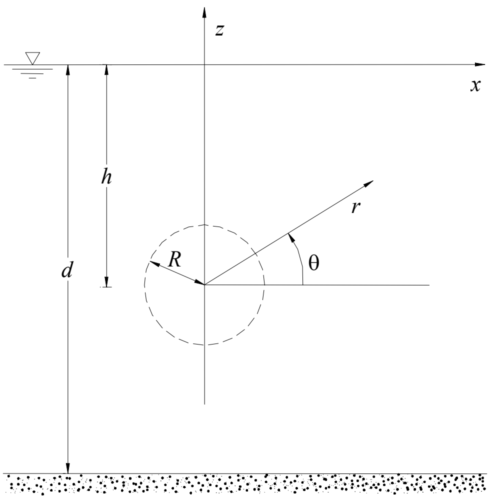


Figure 7. Froude-Krylov force on a horizontal submerged cylinder: the reference frame.

**The narrow-band second-order Froude-Krylov force on a horizontal submerged cylinder**

Let us consider an ideal water-horizontal cylinder with radius $R$ and centre at the level $z=-h$. The Froude-Krylov force components (forces for unitary lenght) are respectively

$$F_x = -\int_0^{2\pi} R\,\Delta p(R,\theta)\cos(\theta)\,\mathrm{d}\theta\,,\quad F_z = -\int_0^{2\pi} R\,\Delta p(R,\theta)\sin(\theta)\,\mathrm{d}\theta \tag{56}$$

where ( $r,\theta$ ) define polar co-ordinates ( $x = r\cos\theta$ , $z = -h + r\sin\theta$ - see Figure 7).

*The horizontal component* $F_x$

Assuming the second-order wave pressure given by expression 48, the narrow-band horizontal component $F_x$ may be written as

$$\begin{aligned} F_x = \mathrm{Re}\Bigg\{ &-\rho g \frac{a e^{-i(wt+\varphi)}}{\cosh(kd)} R \int_0^{2\pi} \cosh[k(d-h+R\sin\theta)]\cdot \\ &\cdot \exp(ikR\cos\theta)\cos\theta\,\mathrm{d}\theta - \rho g \frac{3k a^2 e^{-2i(wt+\varphi)}}{4\sinh^3(kd)\cosh(kd)} R\cdot \\ &\cdot \int_0^{2\pi} \cosh[2k(d-h+R\sin\theta)]\exp(2ikR\cos\theta)\cos\theta\,\mathrm{d}\theta + \\ &+ \rho g \frac{k a^2 e^{-2i(wt+\varphi)}}{4\sinh(kd)\cosh(kd)} R \int_0^{2\pi} \exp(2ikR\cos\theta)\cos\theta\,\mathrm{d}\theta \Bigg\}. \end{aligned} \tag{57}$$

in which $\mathrm{Re}\{x\}$ is the real part of $x$. Analytical integration and some algebra yield

$$\begin{aligned} F_x = &-\rho g \pi k R^2 a \frac{\cosh[k(d-h)]}{\cosh(kd)} \sin(wt+\varphi) - \rho g\, 2\pi k R a^2 \cdot \\ &\left[ kR \frac{3\cosh[2k(d-h)]}{4\sinh^3(kd)\cosh(kd)} - \frac{J_1(2kR)}{4\sinh(kd)\cosh(kd)} \right] \sin[2(wt+\varphi)]\,. \end{aligned} \tag{58}$$

It is easy to verify that the process force $F_x$ (Eq. 58) belongs to the stochastic family $\psi_1$ (Eq. 1), with parameter

$$\delta = -\varepsilon \frac{\dfrac{3\cosh[2k(d-h)]}{\sinh^2(kd)} - \dfrac{J_1(2kR)}{kR}}{\cosh[k(d-h)]\sinh(kd)}\,. \tag{59}$$

In Figure 8 the parameters $\delta / \varepsilon$ as function of $kR$ are shown, for fixed values of $h/d$ and $kd$. Let us note that for fixed radius $R$ the parameter $\delta$ decreases as the depth $d$ increases. The non-linear effects are weak (the parameter $|\delta|$ is smaller than 0.05), so that the process $F_x$ (Eq. 58) may be considered symmetric quasi-Gaussian and the probabilities of exceedance of the absolute maximum and of the absolute minimum (Eq. 36) are very close to the Rayleigh distribution (Figure 3).

*The vertical component* $F_z$

Assuming the second-order wave pressure given by expression 48, the narrow-band vertical component $F_z$ (Eq. 56) may be written as

$$\begin{aligned} F_z = \mathrm{Re}\Bigg\{ &-\rho g \frac{a e^{-i(wt+\varphi)}}{\cosh(kd)} R \int_0^{2\pi} \cosh[k(d-h+R\sin\theta)]\cdot \\ &\cdot \exp(ikR\cos\theta)\sin\theta\,\mathrm{d}\theta - \rho g \frac{3k a^2 e^{-2i(wt+\varphi)}}{4\sinh^3(kd)\cosh(kd)} R\cdot \\ &\cdot \int_0^{2\pi} \cosh[2k(d-h+R\sin\theta)]\exp(2ikR\cos\theta)\sin\theta\,\mathrm{d}\theta + \\ &+ \rho g \frac{ka^2}{2\sinh(2kd)} R \int_0^{2\pi} \cosh[2k(d-h+r\sin\theta)]\sin\theta\,\mathrm{d}\theta \Bigg\}; \end{aligned} \tag{60}$$

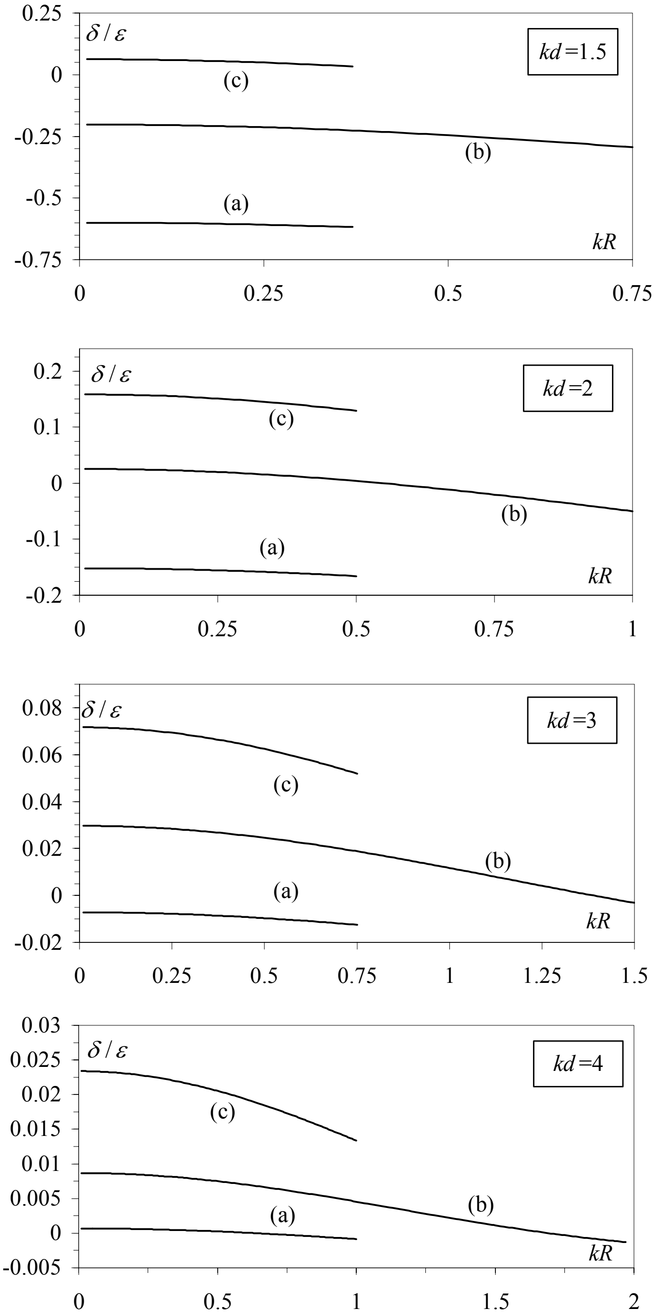


Figure 8. Horizontal component of the Froude-Krylov force on a horizontal submerged cylinder. The parameter $\delta / \varepsilon$ as function of $kR$, for fixed values of $kd$: (a) $h/d = 0.25$; (b) $h/d = 0.50$; (c) $h/d = 0.75$

by solving analytically the integrals in Eq. 60 one gets the following expression of the vertical force component $F_z$

$$F_z = -\rho g \pi k R^2 a \frac{\sinh[k(d-h)]}{\cosh(kd)} \cos(wt+\varphi) - \rho g 2\pi k R a^2 \cdot$$
$$\cdot \left\{ \frac{3k \sinh[2k(d-h)]}{4\sinh^3(kd)\cosh(kd)} \cos[2(wt+\varphi)] - \frac{\sinh[2k(d-h)]}{2\sinh(2kd)} I_1(2kR) \right\} \tag{61}$$

in which $I_1(x)$ is the modified Bessel function of first kind. This process belongs to the stochastic family $\psi_2$ (Eq. 2) with parameters

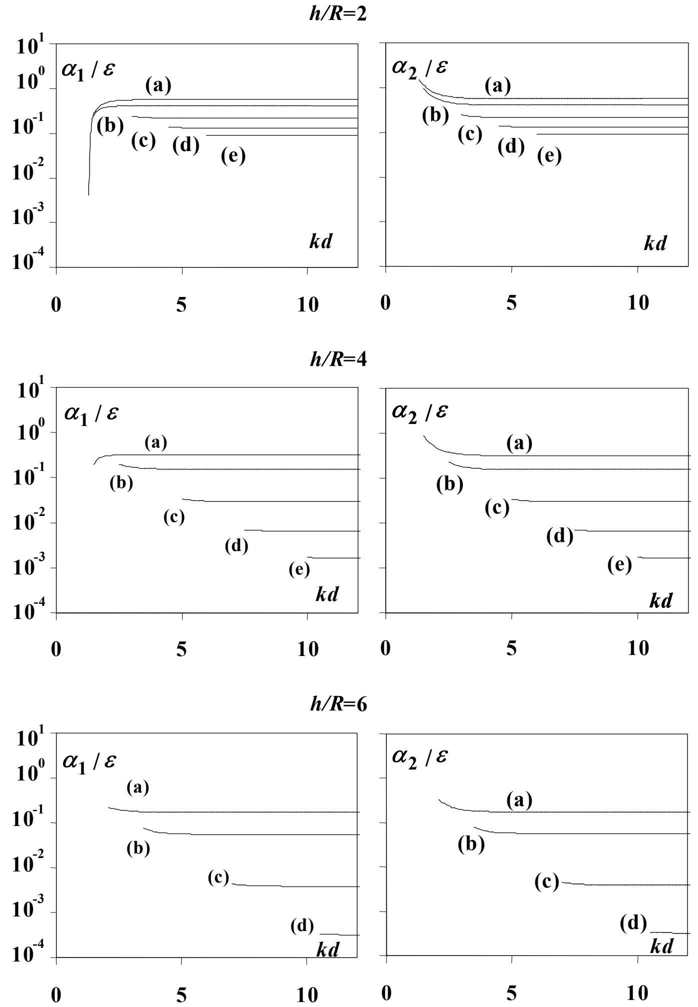


Figure 9. Vertical component of the Froude-Krylov force on a horizontal submerged cylinder: the parameters $\alpha_1 / \varepsilon$ and $\alpha_2 / \varepsilon$ as function of $kd$, for fixed values of $h/R$. (a) $kR = .3$; (b) $kR = .5$; (c) $kR = 1$; (d) $kR = 1.5$; (e) $kR = 2$.

$$\alpha_1 = \varepsilon \frac{\cosh[k(d-h)]}{\sinh(kd)} \left[ -\frac{3}{\sinh^2(kd)} + \frac{I_1(2kR)}{kR} \right]$$
$$\alpha_2 = \varepsilon \frac{\cosh[k(d-h)]}{\sinh(kd)} \left[ \frac{3}{\sinh^2(kd)} + \frac{I_1(2kR)}{kR} \right]. \tag{62}$$

In this case the process is non-symmetric. In Figure 9 the parameters $\alpha_1$ and $\alpha_2$ as function of $kd$ are showed, for fixed values of $h/R$ and $kR$. Let us note that for a fixed depth $kd$ and a fixed $kh$, $\alpha_1$ increases as the radius $kR$ increases; for fixed $kd$ and $kR$, $\alpha_1$ decreases as the $kh$ increases (that is as the cylinder tends to approach the bottom).

Furthermore, from Figure 9 we observe that maximum values of $\alpha_1$ and $\alpha_2$ are within 0.05 and 0.08 (being the maximum value of $\alpha_1 / \varepsilon$ and $\alpha_2 / \varepsilon$ very close to 1).

Finally, being $\alpha_1 > 0$ (in the ranges of values considered in Figure 9), the probabilities of exceedance of the positive peak (absolute maximum) of $F_z$ (Eq. 61) and of the negative peak (absolute minimum) of $F_z$ are different: in particular for a fixed threshold of probability of exceedance, the crest (positive peak) of the wave force $F_z$ are greater than the trough (negative peak). In words for $\alpha_1 > 0$ each realization of the process Froude-Krylov vertical force $F_z$ is a sequence of waves, which have crest amplitude greater than trough amplitude (Figure 4).

**COMPARISON WITH EXPERIMENTAL DATA**

To check our results we have resorted to the file data of the small-scale field experiment of Boccotti (1996) which is relevant to the forces on a horizontal submerged cylinder. Let us start with the horizontal component of the Froude-Krylov force. We have estimated parameter $\delta$ by means of Eq. 52 from the data set of this experiment: the peak period (being necessary to obtain wave number $k$ ), root mean square surface displacement (being necessary to obtain $\varepsilon$ ), water depth $d$ , submergence $h$ of the cylinder centre, radius $R$ of the horizontal cylinder. We have evaluated the value of $\delta$ for each record of the experiment, and these values prove to range between –0.05 and 0.01. In our analytical approach we have shown that the probability of exceedance of the absolute maximum and the probability of exceedance of the absolute minimum are equal to each other and are given by Eq. 36. With $|\delta|$ within 0.05 as in the experiment we are dealing with, Eq. 36 is very close to the Rayleigh form (see Figure 3).

Hence we can expect that both the probability of exceedance of the absolute maximum and the probability of exceedance of the absolute minimum of the horizontal Froude-Krylov force are very close to the Rayleigh form. This is what actually occurs, and can be appreciated from Figure 11.9.*a* of Boccotti (2000).

Let us pass to the vertical component of the Froude-Krylov force. We have estimated the pair $\alpha_1, \alpha_2$ for each record of the experiment by means of Eq. 62. Parameter $\alpha_1$ proves to range between 0.011 and 0.027, and parameter $\alpha_2$ between 0.011 and 0.041. For each pair $\alpha_1, \alpha_2$ we have obtained the probability of exceedance of the absolute maximum and the probability of exceedance of the absolute minimum by means of Eq. 44. The two extreme probabilities of exceedance for the set of pairs $\alpha_1, \alpha_2$ are shown in Figure 10 (lines *a* and *b*). [The upper panel is relevant to the absolute maximum and the lower panel to the absolute minimum.] We see that the probability of exceedance of the absolute maximum (positive peak of $F_z$ ) is greater than the probability of exceedance based on the Rayleigh form. On the contrary, the probability of exceedance of the absolute minimum (negative peak of $F_z$ ) is smaller than the probability of exceedance based on the Rayleigh form. The data points for the probability of exceedance are those of Boccotti (2000) (see his Figure 11.9.*c*), they are relevant to the whole set of record during the experiment, and they clearly confirm the trend of our theoretical predictions.

**REFERENCES**


Arena, F, and Fedele, F (2000*a*). "A narrow-band non-linear stochastic family for the mechanics of sea waves". Department of Mechanics and Materials, Univ. of Reggio Calabria, pp 1-22.

Arena, F, and Fedele, F (2000*b*). "Effects of non-linearity for the wind generated waves". (in Italian*) Atti XXVII Convegno di Idraulica e Costruzioni Idrauliche*, Genova, Vol IV, pp 21-28.

Boccotti, P (1996). "Inertial wave loads on horizontal cylinders: a field experiment", *Ocean Engng*., Vol 23, pp 629-648.

Boccotti, P (2000). "Wave mechanics for ocean engineering". Elsevier Science, pp 1-496.

Borgman, LE (1972). "Statistical models for ocean waves and wave forces", *Advances in Hydroscience*, Vol 8, pp 139-178.

Longuet-Higgins, MS (1952). "On the statistical distribution of the heights of sea waves". *J. Mar. Res*., Vol 11, pp 245-266;

Longuet-Higgins, MS (1963). "The effects of non-linearities on statistical distributions in the theory of sea waves". *J. Fluid Mech*., Vol 17, pp 459-480.

Phillips, OM (1967). "The theory of wind-generated waves". *Advances in Hydroscience*, Vol 4, pp 119-149.

Sarpkaya, T, and Isaacson, M (1981). "Mechanics of wave forces on offshore structures". V. Nostrand Reinhold Comp., New York, pp 1-650.

Tayfun, MA (1980). "Narrow-band nonlinear sea waves". *J. Geophys. Res.*, Vol 85, pp 1548-1552.


(i) distribution of positive peaks

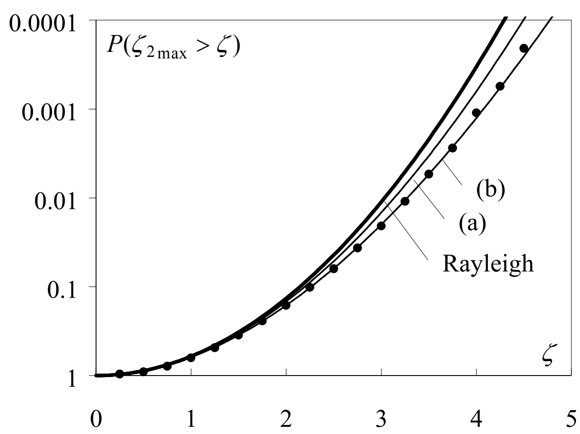


(ii) distribution of negative peaks

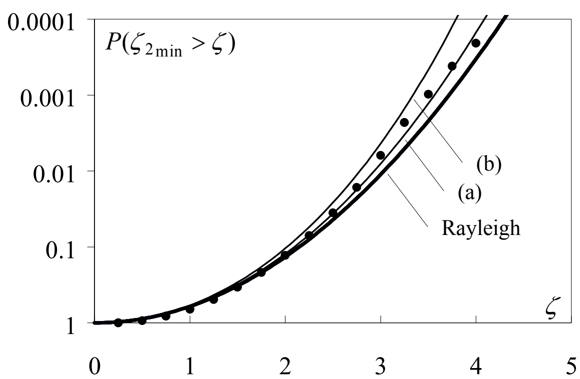


Figure 10. The distributions of the peaks of the vertical Froude-Krylov force on a horizontal submerged cylinder: (i) positive (upward) peak; (ii) negative (downward) peak. Continuous lines are the predictions from Eq. 44: lines (a) are obtained for $\alpha_1$=0.011, lines (b) are obtained for $\alpha_1$=0.041, which are the minimum value and the maximum $\alpha_1$ in the experimental range of $kR$ , $kh$ and $kd$ , assuming $\varepsilon = 0.06$ (the corresponding $\alpha_2$ are equal to 0.011 and 0.041 respectively). Data from Boccotti (2000).